Published in final edited form as:
Arthritis Rheumatol. 2014 March ; 66(3): 637–646. doi:10.1002/art.38279.

In Vivo Luminescent Imaging of NF-κB Activity and Serum Cytokine Levels Predict Pain Sensitivities in a Rodent Model Of Osteoarthritis

Robby D. Bowles, PhD[1], **Brian A. Mata, MD**[2], **Richard D. Bell, BS**[2], **Timothy K. Mwangi, BS**[1], **Janet L. Huebner, MS**[3], **Virginia B. Kraus, MD PhD**[3], and **Lori A. Setton, PhD**[1,2,*]

[1]Dept of Biomedical Engineering, Duke University, Durham, NC

[2]Department of Orthopaedic Surgery, Duke University Medical Center, Durham, NC

[3]Dept of Medicine, Div of Rheumatology, Duke University School of Medicine, Durham, NC

Abstract

Objective—To investigate the relationship between NF-κB activity, cytokine levels, and pain sensitivities in a rodent model of osteoarthritis (OA).

Method—OA was induced in transgenic NF-κB luciferase reporter mice via mono-iodoacetate (MIA) intra-articular injection. Using luminescent imaging we evaluated the temporal kinetics of NF-κB activity and its relationship to the development of pain sensitivities and serum cytokine levels in this model.

Results—MIA induced a transient increase in joint-related NF-κB activity at early time points (day 3 post-injection) and an associated biphasic pain (mechanical allodynia) response. NF-κB activity, serum IL-6, IL-1β, and IL-10 accounted for ~75% of the variability in pain-related mechanical sensitivities in this model. Specifically, NF-κB activity was strongly correlated to mechanical allodynia and serum IL-6 levels in the inflammatory pain phase of this model (day 3), while serum IL-1β was strongly correlated to pain sensitivities in the chronic pain phase of the model (day 28).

Conclusion—Our findings suggest that NF-κB activity, IL-6 and IL-1β may be playing distinct roles in pain sensitivity development in this model of arthritis and may act to distinguish the acute from chronic pain phases of this model. This work establishes luminescent imaging of NF-κB activity as a novel imaging biomarker of pain sensitivities in this model of OA.

Introduction

Knee osteoarthritis (OA) is a leading cause of disability with large associated economic costs. It is anticipated that 20% of adults will be affected by pain or disability associated with OA by the year 2030 (1). At the tissue level, the disease is associated with cartilage degradation, synovial hypertrophy, and subchondral bone remodeling. Clinically, the disease

[*]**Corresponding Address:** Lori A. Setton, Department of Biomedical Engineering, 136 Hudson Hall, Box 90281, Durham, NC 27708, Phone: 919-660-5131, Fax: 919-681-4890, lori.setton@duke.edu.

Authors have no conflicts of interest.

is diagnosed by radiographic changes that include joint space narrowing, presence of osteophytes, and synovial hypertrophy. While patients present with joint pain and impaired joint mobility (2), the mechanistic link between these behaviors and tissue level changes are poorly understood (3–5).

Direct or indirect interactions of inflammatory cytokines (e.g. TNF-α, IL-1β, IL-6) with knee joint afferents has been suggested as a possible contributor to pain in arthritis (6). The inflammatory cytokines TNF-α and IL-6 have been demonstrated to play a direct role in sensitization of nociceptors and the development of mechanical allodynia in preclinical models of inflammatory arthritis (7, 8). Elevated levels of these pro-inflammatory cytokines have been observed in human OA patients (6, 9, 10), while TNF-α and IL-1β ;antagonism may lead to substantial reductions in pain scores for patients presenting with an inflammatory component of osteoarthritis (11–13). While the presentation of inflammation may vary widely across patients with OA and even within the time course of OA pathology, it is now thought that inflammatory cytokines play a key role in pain development in OA.

A key regulator of TNF-α, IL-1β, and IL-6 is the transcription factor nuclear factor kappa-light-chain-enhancer of activated B cells (NF-κB). The NF-κB transcription factor family induces the expression of more than 150 genes that play a role in immunity, inflammation, anti-apotosis, cell proliferation, and the negative feedback of NF-κB (14–17). NF-κB activity can be induced by multiple cellular stimuli including inflammatory cytokines (e.g. TNF-α and IL-1β), extracellular matrix degradation products, and mechanical overload. Once activated, NF-κB induces target gene expression in multiple cell types including synoviocytes, chondrocytes, and fibroblasts (18–20). In arthritis, NF-κB activity is associated with increased expression of pro-inflammatory cytokines (IL-1β, TNF-α, IL-6), metalloproteinases, chemokines, and inducible enzymes (COX-2) (21–24). Although its role in pain in arthritis is not completely understood, the inhibition of key mediators of the NF-κB activation pathway leads to a reduction in pain in rodent models of arthritis (25, 26), suggesting that regulation of these key mediators is the means by which NF-κB facilitates the development and propagation of pain in arthritis.

Carlsen and co-workers previously described the use of a transgenic NF-κB-luciferase reporter mouse to study the transient kinetics of NF-κB activation after UVB radiation exposure and collagen-antibody induced arthritis (17, 27). This transgenic mouse contains NF-κB response elements upstream of the firefly luciferase gene, which allows NF-κB activity to be non-invasively and longitudinally quantified via luminescent imaging; this has been used to demonstrate NF-κB inhibition using a small molecule inhibitor of IKK-2 in a model of collagen antibody-induced arthritis (28).

For its repeatability and rapid onset of pathology, intra-articular injection of mono-iodoacetate (MIA) has been widely used to induce arthritis (26, 29–37). Injection of MIA into the joint inhibits glycolysis in chondrocytes, which results in chondrocyte cell death. As a result, changes resembling human OA that include proteoglycan loss, collagen fibrillation, and subchondral bone remodeling, progress rapidly over a 4–6 week period (29–34, 37, 38). A biphasic pain response has been documented in the MIA model that includes an early inflammation-associated pain phase followed by a late non-inflammatory pain phase (36,

37). The MIA model is of great interest for studying the transient role of NF-κB activity and cytokine levels in contributing to both inflammatory and non-inflammatory pain in a model of OA.

In the present study, *in vivo* luminescent imaging of NF-κB activity was used to investigate the relationship between NF-κB activity, serum cytokines, and pain sensitivities in the rodent model of MIA-induced OA. This model was evaluated to test whether *in vivo* luminescent imaging could provide a spatially accurate measure of NF-κB activity in the knee joint and to test its relationship to development of disease.

Method

Intra-articular Injections and Experimental Timeline

The transgenic mice used for this study were engineered to carry cDNA for firefly luciferase downstream of NF-kB response elements (n=24, BALB/c-Tg(NFκB-RE-luc), age 7–8 weeks; Taconic Farms Inc., Hudson, NY). All procedures were performed with approval of the Duke University IACUC. Following a 1-week acclimation period, under anesthesia (2% isoflurane inhalation), mice received intra-articular knee injections via 30-gauge needle of MIA (5 μl, 10 mg/ml, n=12) or saline as a control (5 μl, n=12). One set of animals (n=6/group, Saline and MIA) was sacrificed on day 3 and a second set of animals was sacrificed on day 28 (n=6/group, Saline and MIA). Time points of sacrifice were selected to coincide with the early (day 3) and late (day 28) pain phases observed in the MIA model. Prior to sacrifice, animals underwent *in vivo* luminescent imaging to quantify NF-κB activity pre-MIA injection and on days 1, 3, 7, 14, 21, and 28 post-MIA injection. Mice underwent testing to measure mechanical allodynia and relative weight-bearing at these same time points. In a subset of animals, organs and relevant tissues were harvested for *ex vivo* imaging immediately after sacrifice. Serum was obtained from all animals at sacrifice (day 3 or day 28) via cardiac puncture to assay for a subset of systemic pro- and anti- inflammatory cytokines.

In Vivo NF-κB Activity Luminescent Imaging

At each imaging time point, mice were anesthetized and injected with D-luciferin prior to imaging (150 mg/kg i.p., Caliper Life Sciences Inc., Hopkinton, MA). After 10 minutes to allow D-luciferin distribution, whole-body imaging of luminescence arising from NF-κB activity was performed on an *in vivo* imaging system (IVIS 100, Perkin Elmer, Waltham, Massachusetts) with a 15 second exposure; determined from preliminary studies to avoid saturation of pixels in all images.

Six cadaveric mice were used to define an appropriate region of interest (ROI) for luminescence image analysis. Radiographs of cadaveric mice were obtained on an *In Vivo* Imaging System (IVIS) FX Pro (Carestream Health Inc., Rochester, NY) using the same positioning as for luminescent imaging. An ROI was selected (4 × 8 mm ellipse) that was anchored to the intersection of the ipsilateral hind limb and mouse body (Figure 1A) and encompassed the total knee joint of all animals.

At each time point, the ROI luminescence (LUM_{ROI}) was measured as photons/sec/cm^2 for all animals. Luminescence data for each animal at each time point was normalized to preinjection values from the same animal (N_{LUM}) according to equation 1,

$$N_{LUM} = \frac{LUM_{ROI}}{(LUM_{ROI})_{preinjection}}. \quad (1)$$

Ex Vivo NF-κB Activity Luminescent Imaging

Immediately post sacrifice, the ipsilateral and contralateral tibiofemoral knee joints, patella, and adjacent muscle tissue were harvested for immediate *ex vivo* luminescent imaging in a subset of animals (n=18). Tissue was placed in separate wells of a 12-well tissue culture plate and each well was supplemented with 300 μg/ml D-luciferin in Dulbecco's Phosphate-Buffered Saline (Gibco, Grand Island, New York). After 5 minutes, the tissue culture plate was imaged as for the whole body on the IVIS100 (Perkin Elmer; 15 second exposure). Selected ROI around each tissue was measured as photons/sec/cm^2 (LUM_{KNEE}, $LUM_{PATELLA}$, LUM_{MUSCLE}).

Pain-related Sensitivity (Mechanical Allodynia)

Mice were acclimated to a wire-bottom cage and exposed to the von Frey testing procedure over a period of 3 days prior to the start of the experiment. Mechanical allodynia was evaluated in the ipsilateral hind paw by touching the plantar surface with von Frey filaments (0.07 – 4.0 g; Stoelting, Wood Dale, Illinois) using the "up-down" method (39). Briefly, filaments ranging from 0.07 g to 4.0 g were applied to the ipsilateral hind paw for 3–4 seconds, starting with the 0.6 g filament. A positive response (paw flick, lick, or vocalization) resulted in moving to the next weaker filament, while a lack of response resulted in moving to the next stronger filament. Data for paw withdrawals following filament application for a minimum of four filaments was used to calculate the 50% withdrawal threshold in units of gram-force (50%WT). Data were collected pre-injection and on days 3, 7, 14, 21, and 28 post-injection and normalized to the pre-injection levels of the same animal and limb ($N_{50\%WT}$); data are presented as a percentage of the pre-injection 50%WT according to equation 2,

$$N_{50\%WT} = \frac{50\%WT}{50\%WT_{preinjection}} \times 100. \quad (2)$$

Weight-Bearing

Mouse hind-limb weight-bearing was determined using an incapacitance meter (IITC Life Science Inc., Woodland Hills, CA). Mice were placed in an angled plexiglass chamber with the two hind paws resting on two independent force plates, the front paws resting on the plexiglass ramp, and the mouse facing forward. Force (gram-force) readings were obtained over a 3 second interval for both the ipsilateral (WB_{ipsi}) and contralateral (WB_{contr}) limb; three independent measurements were obtained for each mouse at each time point and averaged. Percentage weight-bearing was normalized (N_{WB}) by dividing the weight-bearing

on the ipsilateral limb by the total weight-bearing for both hindlimbs according to equation 3,

$$N_{WB}=\frac{WB_{ipsi}}{WB_{ipsi}+WB_{contr}}\times 100. \quad (3)$$

Serum Cytokines

The following serum cytokine concentrations were quantified using multiplex and single immunoassays (Mouse Pro-inflammatory 7-plex and Mouse MCP-1 single-plex, Meso Scale Discovery, Rockville, MD): interleukin-1 beta (IL-1β), interleukin-6 (IL-6), interleukin-10 (IL-10), interleukin-12p70 (IL-12p70), chemokine C-X-C motif ligand 1 (CXCL1), tumor necrosis factor-alpha (TNF-α), interferon-gamma (IFN-γ), and monocyte chemotactic protein-1 (MCP-1). Measurements were performed on a SECTOR Imager 2400 (Meso Scale Discovery, Rockville, MD). The mean intra-assay CVs for the 7-plex pro-inflammatory and MCP-1 immunoassay were 3.3% and 2.8%, respectively. The lower limit of detection (LLOD) for each cytokine is as follows: IL-1β (0.21 pg/ml), IL-6 (3.07 pg/ml), IL-10 (0.37 pg/ml), IL-12p70 (9.73 pg/ml), CXCL1 (0.27 pg/ml), TNF-α (0.63 pg/ml), IFN-γ (0.06 pg/ml), and MCP-1 (1.46 pg/ml). One half of the LLOD was used for any value below the level of detection for the purpose of performing statistical analyses. Concentrations of serum TNF-α and IL-12p70 were below the LLOD in a majority of samples and so were not included in the analysis.

Histology

Both ipsilateral and contralateral limbs were dissected to remove excess skin and musculature while preserving the knee joint capsule. The intact joints were fixed in 10% formalin for 3 days, decalcified for 5 days in Cal-EX Decalcifying Solution (Fisher Scientific, Hampton, NH), and embedded in paraffin. Sections (8 μm thick) were taken in the coronal plane within the load-bearing region of the joint and mounted at 80 μm intervals. Three slides covering the central sections of each joint were stained with Safranin-O and fast green. A single section representing the most severe evidence of arthritic changes was selected for each joint and was scored according to a modified Mankin scoring system (40). Images were randomized and two blinded scorers (BAM, RDB) assigned grades, by consensus, to the tibial and femoral cartilage in the medial and lateral compartments. Ordinal scores were assigned for 7 parameters related to degeneration including cartilage structure (score range 0–11), loss of Safranin-O staining (range 0–8), tidemark duplication (range 0–3), fibrocartilage formation (range 0–2), chondrocyte clones in uncalcified cartilage (range 0–2), hypertrophic chondrocytes in calcified cartilage (range 0–2), and subchondral bone thickness (range 0–2). Scores were summed for the lateral femur, medial femur, lateral tibia, and medial tibia to arrive at a maximum score of 120 for each knee.

Statistics

All statistical analyses were performed using JMP Pro (JMP, Cary, NC). Continuous, normally distributed data ($N_{50\%WT}$, N_{WB}, N_{LUM}) were analyzed by two-way analysis of variance (ANOVA) with Tukey post hoc test, treating day and group (MIA, Saline) as

factors. Significance was tested at $\alpha = 0.05$. Ordinal (Mankin score) and non-normally distributed data (serum cytokines) were analyzed by a Friedman test. *Post-hoc* analysis with Wilcoxon Signed-Rank Tests was conducted with a Bonferroni correction of $\alpha = 0.008$ (0.05/6).

To test for hypothesized relationships between NF-κB activity (N_{LUM}), serum cytokines (IL-6, CXCL1, IL-1β, MCP-1, IFN-γ, and IL-10), and pain-related measures ($N_{50\%WT}$, N_{WB}), multivariate linear regression was performed using both day 3 and day 28 data (all measures collected on these days) for both MIA and saline groups. Significance of the regressions were reported with a Bonferroni correction of $\alpha = 0.001$ (0.05/45). All variables except $N_{50\%WT}$, N_{WB} were log-transformed (base-10) prior to statistical analysis.

To test for the ability of NF-κB activity luminescent imaging and serum cytokine measures to account for pain-related sensitivity in the MIA model, $N_{50\%WT}$ and N_{WB} were modeled using partial least squares regression to produce a linear model from the log-transformed variables NLUM, IL-6, CXCL1, IL-1β, MCP-1, IFN-γ, and IL-10. A threshold for variable influence on projection (VIP) was set at 0.8 for inclusion in the final linear model (41). The VIP parameter is a summarizing tool that describes the relative importance of the predictors in order to rank the importance of each *X* in relation to a chosen response variable. Both VIP and scaled and centered regression coefficients are reported for independent variables included in the final model. K-fold cross validation with 6 subsamples was used to calculate Q^2, an estimate of the predictive power of the models.

To test for relationships that were specific to pain phase (early (day 3) or late (day 28)), additional multivariate linear regressions were performed to test for an association of 50% withdrawal threshold ($N_{50\%WT}$) with independent variables (N_{LUM}, IL-6, IL-1β, and IL-10) at day 3 or 28. Significance of the regression was reported with a Bonferroni correction of $\alpha = 0.0125$ (0.05/4) applied for both days 3 and 28. Linear regression was performed to test for an association of weight-bearing (N_{WB}) at day 3 or day 28 with independent variables (N_{LUM}, IL-6, CXCL1, and MCP-1). Significance of the regression was reported $\alpha = 0.0125$ (0.05/4) for both days 3 and 28. Independent variables were log-transformed (base-10) prior to statistical analysis.

Results

NF-κB Activity in MIA

A transient increase in NF-κB activity luminescence (N_{LUM}) (~4–5 fold) was observed following MIA injection into the knee joint (Figure 1B and C). Luminescence was observed consistently and broadly distributed in the MIA injected limb on day 1. Over time, the intensity of luminescence, which peaked at the knee ROI day 1 post-injection, slowly and steadily declined thereafter (Figure 1B). For MIA injected knees, luminescence (N_{LUM}) was significantly increased in the knee ROI compared to pre-injection values on days 1 ($p<0.0001$) and 3 ($p<0.0001$; ANOVA) (Figure 1C), but returned to pre-injection levels by day 28. Additionally, luminescence (N_{LUM}) was significantly increased in MIA injected knees compared to saline injected knees on day 3 ($p=0.043$; ANOVA).

Ex Vivo NF-κB Activity Luminescent Imaging

In vivo luminescence (LUM_{ROI}) was significantly correlated to the *ex vivo* tibiofemoral knee luminescence (LUM_{KNEE}) ($R^2 = 0.71$, $p<0.0001$), and *ex vivo* patella luminescence ($LUM_{PATELLA}$) ($R^2 = 0.52$, $p<0.0001$), with evidence of weaker correlations to *ex vivo* muscle luminescence (LUM_{MUSCLE}) ($R^2 = 0.16$, $p<0.016$) (Figure 2). This observation confirms the tibiofemoral knee as the primary source of *in vivo* NF- κB generated luminescence.

Serum Cytokines

Serum levels of IL-6 were transiently increased following MIA injection into the knee joint (Figure 3). Serum IL-6 was significantly increased in MIA injected animals compared to saline injected animals on day 3 ($p=0.004$) and significantly increased on day 3 compared to day 28 in MIA injected animals ($p<0.0001$; Friedman Test). There was no evidence of between group or time-related differences in serum cytokines CXCL1, MCP-1, IFN-γ, IL-1β, IL-10 ($p > 0.05$; Friedman Test).

Histological Evidence of Arthritis

Histological scoring indicated that MIA injected knees showed the greatest change in proteoglycan loss, fibrillation/clefts of the articular cartilage surface, and hypertrophic chondrocytes in the calcified cartilage (Figure 4A). On day 28, there was evidence of statistically significant differences in the total modified Mankin score in MIA injected limbs compared to saline injected limbs ($p=0.005$; Friedman Test) (Figure 4B).

Behavioral Assessments

MIA knee injection resulted in the induction of significantly elevated sensitivity to mechanical stimuli (allodynia) in the ipsilateral limb (Figure 4 C, D). Compared to saline injected hindlimbs, the 50% withdrawal threshold ($N_{50\%WT}$) normalized to pre-injection values was significantly decreased for MIA injected hindlimbs on days 3 ($p<0.0001$), 7 ($p=0.0043$), 21 ($p=0.0021$), and 28 ($p=0.0033$; ANOVA), and significantly decreased in MIA injected limbs compared to pre-injection levels on days 3 ($p<0.0001$) and 7 ($p<0.0001$; ANOVA) (Figure 4C).On day 28, MIA injected limbs showed a trend for decreased $N_{50\%WT}$ compared to pre-injection levels, but failed to reach the threshold for statistical significance ($p=0.082$; ANOVA). The percent of weight-bearing on the ipsilateral limb significantly decreased in MIA injected limbs on days 3 ($p=0.0002$) and 7 ($p=0.035$; ANOVA) compared to pre-injection values and day 3 ($p=0.023$; ANOVA) compared to saline injection (Figure 5D).

Relationships Between NF-κB Activity, Serum Cytokines, and Pain-Related Sensitivities

NF-κB activity, serum cytokines, and the pain-related sensitivities (Figure 5 and 6) were all significantly associated in the MIA model. After adjusting for multiple comparisons by Bonferroni correction, multivariate linear regression identified a correlation for NF-κB activity (luminescence) and pain-related sensitivity data when analyzed independently of pain phase (i.e. early (day 3) and late (day 28)). NF-κB activity (N_{LUM}) was strongly negatively correlated to the 50% withdrawal threshold ($N_{50\%WT}$) ($r = -0.70$, $p=<0.0001$)

(Figure 5). No evidence of additional significant correlations was detected between NF-κB activity (N_{LUM}), mechanical allodynia ($N_{50\%WT}$), weight-bearing (N_{WB}), and serum levels of IL-6, CXCL1, IL-1β, MCP-1, IFN-γ, and IL-10 when analyzed independently of pain phase.

A linear model was constructed for mechanical allodynia ($N_{50\%WT}$) and weight-bearing (N_{WB}) using the non-invasive measure of NF-κB activity (N_{LUM}) and serum cytokines (Figure 6A). The model for mechanical allodynia described ~75% (R^2) of the variability in mechanical allodynia ($N_{50\%WT}$) using the variables N_{LUM} (VIP = 1.7), IL-6 (VIP = 1.3), IL-1β (VIP = 0.8), and IL-10 (VIP = 0.9). Using K-fold cross validation the model was able to predict ~67% (Q^2) of the variability in the data. The model for weight bearing described ~27% (R^2) of the variability in weight bearing (N_{WB}) using the variables N_{LUM} (VIP = 1.6), IL-6 (VIP = 1.3), CXCL1 (VIP = 1.3), and MCP-1 (VIP = 1.1). However, using K-fold cross validation the model was able to predict only ~7% (Q^2) of the variability in the data.

Of the significant parameter estimates observed in the general linear model, only NF-κB related luminescence (N_{LUM}) was significantly correlated to mechanical allodynia ($N_{50\%WT}$) when analyzed independently of pain phase (Figure 5). Multivariate correlations were conducted to compare the significant variables in the linear models to mechanical allodynia and weight-bearing by day. Adjusting for multiple comparisons, luminescence (N_{LUM}) and the 50% withdrawal threshold ($N_{50\%WT}$) were strongly negatively correlated ($r = -0.78$, $p=0.0029$) on day 3, serum IL-6 and $N_{50\%WT}$ were strongly negatively correlated ($r=-0.67$, $p=0.011$) on day 3, and serum IL-1β and $N_{50\%WT}$ were strongly negatively correlated ($r=-0.72$, $p=0.0088$) on day 28 (Figure 6B). NF-κB activity (N_{LUM}) and ipsilateral weight-bearing (N_{WB}) were also strongly negatively correlated ($r=-0.71$, $p=0.012$) on day 3 (Figure 6C).

Discussion

We used luminescent imaging to investigate the relationship between NF-κB activity, cytokine levels, and pain sensitivities in a rodent model of OA. The tibiofemoral knee appeared to be the principal source of NF-κB related luminescence following MIA injection, and revealed strong relationships between local measures of NF-κB activity, pain sensitivity, and systemic measures of IL-6. These findings establish luminescent imaging of NF-κB activity as a novel imaging biomarker of pain-related sensitivities in a rodent model of OA.

Injection of MIA into the NF-κB-luc reporter mice produced both histological and behavioral changes associated with the development of arthritis (26, 35). Significant histological changes were observed in the MIA injected knees by day 28. A biphasic pain response was observed with an acute increase in mechanical sensitivity followed by a persistent increase in MIA injected limbs compared to saline control limbs on days 21 and 28. Similar biphasic pain responses that include an early inflammation associated pain phase and a late non-inflammation associated pain phase have been reported in weight bearing and spontaneous mobility in the MIA model (36, 37). Thus, the biphasic response observed in

the mechanical sensitivity data is consistent with these previous pain-related behavioral measures.

The biphasic response has been reported in the rat model at moderate MIA injection concentrations (6 – 60 mg/ml) (36, 37), while high concentrations (50–100 mg/ml) produce a pain response that is characterized by rapid onset, no recovery, and is sustained chronically in both mice and rats (33, 44, 45). The concentration used within this study (10 mg/ml) was within the range expected to produce a biphasic pain response. It is important to note that, while present, the late pain phase observed in this study was moderate and was only observed in the mechanical allodynia measure. A more severe chronic pain response in both mechanical allodynia and weight bearing would have likely been observed at higher concentrations of MIA injection.

Luminescent *in vivo* imaging provides a powerful tool to non-invasively quantify molecular events during musculoskeletal disease progression and therapeutic intervention. NF-κB activity was observed in the *ex vivo* tibiofemoral knee and patella with a strong correlation with the *in vivo* ROI luminescence measurements. The *ex vivo* imaging established the tibiofemoral knee, and to a lesser extent the patella, as the sources of the *in vivo* total knee ROI luminescence. *In vivo* luminescent imaging as used here, provided a spatially accurate measure of NF-κB activity in the knee that may be useful for the rapid screening of NF-κB targeting therapeutics for the treatment of OA and other inflammatory pathologies (18, 42).

MIA injection induced a transient increase in NF-κB activity that preceded histological changes in the knee. Immediately post injection, elevated NF-κB activity was observed throughout the limb on day 1, which localized to the knee by day 3, and returned to pre-injection levels by day 28. This pattern was consistent with the pattern previously reported for MIA injection, namely an inflammatory response in the first 1–3 days post-injection, followed by a subsequent dissipation of inflammation (29, 30). Additionally, NF-κB activity has been demonstrated during inflammation in models of collagen-induced and adjuvant-induced arthritis (28, 43). A peak in joint swelling at day 1, a peak in synovial hyperplasia at day 3, and synovial inflammatory cell invasion characterizes this inflammatory response through day 3 in the MIA model. It is possible that the day 3 time point chosen for this study may have missed the peak levels of inflammation and pain sensitivity, but the elevated NF-κB activity/IL-6 levels at day 3 indicate that this time point falls within the inflammatory period of this model. Our data suggest that the primary role of NF-κB in the MIA model is as a mediator of the early inflammatory response and may suggest that NF-κB targeted therapeutics would be most effective during the early developmental phases of OA.

In this study, luminescent imaging of NF-κB activity and NF-κB regulated serum cytokines were validated as biomarkers of pain-related sensitivities in the MIA model. NF-κB activity was very strongly correlated to mechanical allodynia and was the only measure with significant correlation to mechanical allodynia when analyzed independently of pain phase. A linear model was constructed that was capable of predicting ~67% (Q^2) of the variability in the mechanical allodynia data, which included luminescent imaging of NF-κB activity, serum IL-6, serum IL-1β, and serum IL-10 as predictive variables. NF-κB activity was determined as the most important variable in the model according to VIP. When these

measures were correlated to mechanical allodynia by pain phase, NF-κB activity and serum IL-6 were strongly correlated to mechanical sensitivities in the early pain phase and IL-1β was strongly correlated to mechanical sensitivities in the late pain phase. These data support the presence of an early inflammatory pain phase and a late non-inflammatory pain phase in the MIA model of OA and suggests distinct biomarkers can distinguish the two phases. It may indicate a distinct role for the NF-κB /IL-6 pathway in the acute pain sensitivities in arthritis and IL-1β in chronic pain sensitivities associated with joint/cartilage destruction. This is consistent with previous findings that both IL-6 and IL-1β are associated with increased pain sensitivities in the rodent knee joint (7, 46). Overall, the luminescent imaging of NF-κB activity and serum cytokine measures suggest utility as a panel of non-invasive biomarkers of pain-related sensitivities in the MIA model with biomarker subsets unique for distinguishing the distinct pain phases.

This study demonstrates the use of non-invasive *in vivo* luminescent imaging to measure NF-κB activity in a mouse model of osteoarthritis and the comparison of key molecular events in arthritis to pain sensitivity development. MIA injection induced a transient increase in NF-κB activity at early time points in the tibiofemoral joint, which was correlated with developing pain sensitivities in this model of OA. NF-κB activity and serum IL-6 were specifically related to the inflammation-associated acute pain phase and IL-1β with the late pain phase following MIA injection. The demonstrated relationship between NF-κB activity, a subset of serum cytokines (i.e. IL-6, IL-1β, and IL-10), and mechanical allodynia suggests the use of NF-κB luminescent imaging with serum cytokines as non-invasive biomarkers of pain sensitivities in this model. It will be important in future work to test how these results translate to human OA and it is important to note that the transgenic nature of the luminescent imaging of NF-κB activity makes this imaging a challenge in the clinical setting. These data suggest the feasibility and utility of luminescent imaging of NF-κB for rapid screening of targeted NF-κB antagonists for treating knee OA and other pathologies driven by NF-κB.

Acknowledgments

This work was completed with support from NIH Grants F32 AR063012, F31 AR063610, R01 AR047442, and P01 AR050245. The authors thank Stephen Johnson for his assistance with the surgical procedures and Gregory Palmer for guidance on experiments with IVIS imaging.

References

1. Henrotin Y, Clutterbuck AL, Allaway D, Lodwig EM, Harris P, Mathy-Hartert M, et al. Biological actions of curcumin on articular chondrocytes. Osteoarthritis Cartilage. 2010; 18(2):141–149. [PubMed: 19836480]
2. Hinton R, Moody RL, Davis AW, Thomas SF. Osteoarthritis: diagnosis and therapeutic considerations. Am Fam Physician. 2002; 65(5):841–848. [PubMed: 11898956]
3. Hannan MT, Felson DT, Pincus T. Analysis of the discordance between radiographic changes and knee pain in osteoarthritis of the knee. J Rheumatol. 2000; 27(6):1513–1517. [PubMed: 10852280]
4. Neogi T, Felson D, Niu J, Nevitt M, Lewis CE, Aliabadi P, et al. Association between radiographic features of knee osteoarthritis and pain: results from two cohort studies. BMJ. 2009; 339:b2844. [PubMed: 19700505]

5. Bedson J, Croft PR. The discordance between clinical and radiographic knee osteoarthritis: a systematic search and summary of the literature. BMC Musculoskelet Disord. 2008; 9:116. [PubMed: 18764949]
6. Kapoor M, Martel-Pelletier J, Lajeunesse D, Pelletier JP, Fahmi H. Role of proinflammatory cytokines in the pathophysiology of osteoarthritis. Nat Rev Rheumatol. 2011; 7(1):33–42. [PubMed: 21119608]
7. Boettger MK, Leuchtweis J, Kummel D, Gajda M, Brauer R, Schaible HG. Differential effects of locally and systemically administered soluble glycoprotein 130 on pain and inflammation in experimental arthritis. Arthritis Res Ther. 2010; 12(4):R140. [PubMed: 20626857]
8. Boettger MK, Hensellek S, Richter F, Gajda M, Stockigt R, von Banchet GS, et al. Antinociceptive effects of tumor necrosis factor alpha neutralization in a rat model of antigen-induced arthritis: evidence of a neuronal target. Arthritis Rheum. 2008; 58(8):2368–2378. [PubMed: 18668541]
9. Schlaak JF, Pfers I, Meyer Zum Buschenfelde KH, Marker-Hermann E. Different cytokine profiles in the synovial fluid of patients with osteoarthritis, rheumatoid arthritis and seronegative spondylarthropathies. Clin Exp Rheumatol. 1996; 14(2):155–162. [PubMed: 8737721]
10. Farahat MN, Yanni G, Poston R, Panayi GS. Cytokine expression in synovial membranes of patients with rheumatoid arthritis and osteoarthritis. Ann Rheum Dis. 1993; 52(12):870–875. [PubMed: 8311538]
11. Bacconnier L, Jorgensen C, Fabre S. Erosive osteoarthritis of the hand: clinical experience with anakinra. Ann Rheum Dis. 2009; 68(6):1078–1079. [PubMed: 19435727]
12. Grunke M, Schulze-Koops H. Successful treatment of inflammatory knee osteoarthritis with tumour necrosis factor blockade. Ann Rheum Dis. 2006; 65(4):555–556. [PubMed: 16531556]
13. Fioravanti A, Fabbroni M, Cerase A, Galeazzi M. Treatment of erosive osteoarthritis of the hands by intra-articular infliximab injections: a pilot study. Rheumatol Int. 2009; 29(8):961–965. [PubMed: 19198842]
14. Roman-Blas JA, Jimenez SA. NF-kappaB as a potential therapeutic target in osteoarthritis and rheumatoid arthritis. Osteoarthritis Cartilage. 2006; 14(9):839–848. [PubMed: 16730463]
15. Simmonds RE, Foxwell BM. Signalling, inflammation and arthritis: NF-kappaB and its relevance to arthritis and inflammation. Rheumatology (Oxford). 2008; 47(5):584–590. [PubMed: 18234712]
16. Marcu KB, Otero M, Olivotto E, Borzi RM, Goldring MB. NF-kappaB signaling: multiple angles to target OA. Current drug targets. 2010; 11(5):599–613. [PubMed: 20199390]
17. Carlsen H, Alexander G, Austenaa LM, Ebihara K, Blomhoff R. Molecular imaging of the transcription factor NF-kappaB, a primary regulator of stress response. Mutat Res. 2004; 551(1–2):199–211. [PubMed: 15225593]
18. Roman-Blas JA, Jimenez SA. NF-kappaB as a potential therapeutic target in osteoarthritis and rheumatoid arthritis. Osteoarthritis Cartilage. 2006; 14(9):839–848. [PubMed: 16730463]
19. Aupperle K, Bennett B, Han Z, Boyle D, Manning A, Firestein G. NF-kappa B regulation by I kappa B kinase-2 in rheumatoid arthritis synoviocytes. J Immunol. 2001; 166(4):2705–2711. [PubMed: 11160335]
20. Fujisawa K, Aono H, Hasunuma T, Yamamoto K, Mita S, Nishioka K. Activation of transcription factor NF-kappa B in human synovial cells in response to tumor necrosis factor alpha. Arthritis Rheum. 1996; 39(2):197–203. [PubMed: 8849369]
21. Pulai JI, Chen H, Im HJ, Kumar S, Hanning C, Hegde PS, et al. NF-kappa B mediates the stimulation of cytokine and chemokine expression by human articular chondrocytes in response to fibronectin fragments. J Immunol. 2005; 174(9):5781–5788. [PubMed: 15843581]
22. Forsyth CB, Cole A, Murphy G, Bienias JL, Im HJ, Loeser RF Jr. Increased matrix metalloproteinase-13 production with aging by human articular chondrocytes in response to catabolic stimuli. J Gerontol A Biol Sci Med Sci. 2005; 60(9):1118–1124. [PubMed: 16183949]
23. Benito MJ, Murphy E, Murphy EP, van den Berg WB, FitzGerald O, Bresnihan B. Increased synovial tissue NF-kappa B1 expression at sites adjacent to the cartilage-pannus junction in rheumatoid arthritis. Arthritis Rheum. 2004; 50(6):1781–1787. [PubMed: 15188354]
24. Handel ML, McMorrow LB, Gravallese EM. Nuclear factor-kappa B in rheumatoid synovium. Localization of p50 and p65. Arthritis Rheum. 1995; 38(12):1762–1770. [PubMed: 8849348]

25. Ahmed AS, Li J, Ahmed M, Hua L, Yakovleva T, Ossipov MH, et al. Attenuation of pain and inflammation in adjuvant-induced arthritis by the proteasome inhibitor MG132. Arthritis Rheum. 2010; 62(7):2160–2169. [PubMed: 20506183]
26. Ahmed AS, Li J, Erlandsson-Harris H, Stark A, Bakalkin G, Ahmed M. Suppression of pain and joint destruction by inhibition of the proteasome system in experimental osteoarthritis. Pain. 2012; 153(1):18–26. [PubMed: 22018973]
27. Carlsen H, Moskaug JO, Fromm SH, Blomhoff R. In vivo imaging of NF-kappa B activity. J Immunol. 2002; 168(3):1441–1446. [PubMed: 11801687]
28. Izmailova ES, Paz N, Alencar H, Chun M, Schopf L, Hepperle M, et al. Use of molecular imaging to quantify response to IKK-2 inhibitor treatment in murine arthritis. Arthritis Rheum. 2007; 56(1):117–128. [PubMed: 17195214]
29. van der Kraan PM, Vitters EL, van de Putte LB, van den Berg WB. Development of osteoarthritic lesions in mice by "metabolic" and "mechanical" alterations in the knee joints. Am J Pathol. 1989; 135(6):1001–1014. [PubMed: 2556924]
30. van Osch GJ, van der Kraan PM, van den Berg WB. Site-specific cartilage changes in murine degenerative knee joint disease induced by iodoacetate and collagenase. J Orthop Res. 1994; 12(2):168–175. [PubMed: 8164088]
31. Janusz MJ, Hookfin EB, Heitmeyer SA, Woessner JF, Freemont AJ, Hoyland JA, et al. Moderation of iodoacetate-induced experimental osteoarthritis in rats by matrix metalloproteinase inhibitors. Osteoarthritis Cartilage. 2001; 9(8):751–760. [PubMed: 11795995]
32. Guzman RE, Evans MG, Bove S, Morenko B, Kilgore K. Mono-iodoacetate-induced histologic changes in subchondral bone and articular cartilage of rat femorotibial joints: an animal model of osteoarthritis. Toxicol Pathol. 2003; 31(6):619–624. [PubMed: 14585729]
33. Fernihough J, Gentry C, Malcangio M, Fox A, Rediske J, Pellas T, et al. Pain related behaviour in two models of osteoarthritis in the rat knee. Pain. 2004; 112(1–2):83–93. [PubMed: 15494188]
34. Schuelert N, McDougall JJ. Grading of monosodium iodoacetate-induced osteoarthritis reveals a concentration-dependent sensitization of nociceptors in the knee joint of the rat. Neurosci Lett. 2009; 465(2):184–188. [PubMed: 19716399]
35. Liu P, Okun A, Ren J, Guo RC, Ossipov MH, Xie J, et al. Ongoing pain in the MIA model of osteoarthritis. Neurosci Lett. 2011; 493(3):72–75. [PubMed: 21241772]
36. Bove SE, Calcaterra SL, Brooker RM, Huber CM, Guzman RE, Juneau PL, et al. Weight bearing as a measure of disease progression and efficacy of anti-inflammatory compounds in a model of monosodium iodoacetate-induced osteoarthritis. Osteoarthritis Cartilage. 2003; 11(11):821–830. [PubMed: 14609535]
37. Guingamp C, Gegout-Pottie P, Philippe L, Terlain B, Netter P, Gillet P. Mono-iodoacetate-induced experimental osteoarthritis: a dose-response study of loss of mobility, morphology, and biochemistry. Arthritis Rheum. 1997; 40(9):1670–1679. [PubMed: 9324022]
38. Henriksen M, Graven-Nielsen T, Aaboe J, Andriacchi TP, Bliddal H. Gait changes in patients with knee osteoarthritis are replicated by experimental knee pain. Arthritis Care Res (Hoboken). 62(4): 501–509. [PubMed: 20391505]
39. Chaplan SR, Bach FW, Pogrel JW, Chung JM, Yaksh TL. Quantitative assessment of tactile allodynia in the rat paw. J Neurosci Methods. 1994; 53(1):55–63. [PubMed: 7990513]
40. Furman BD, Strand J, Hembree WC, Ward BD, Guilak F, Olson SA. Joint degeneration following closed intraarticular fracture in the mouse knee: a model of posttraumatic arthritis. J Orthop Res. 2007; 25(5):578–592. [PubMed: 17266145]
41. Eriksson L, Johansson N, Kettaneh-Wold N, Trygg J, Wikstrom C, Wold S. Multi- and Megavariate Data Analysis. Umea: Umetrics AB. 2006
42. Gupta SC, Sundaram C, Reuter S, Aggarwal BB. Inhibiting NF-kappaB activation by small molecules as a therapeutic strategy. Biochim Biophys Acta. 2010; 1799(10–12):775–787. [PubMed: 20493977]
43. Eguchi J, Koshino T, Takagi T, Hayashi T, Saito T. NF-kappa B and I-kappa B overexpression in articular chondrocytes with progression of type II collagen-induced arthritis in DBA/1 mouse knees. Clin Exp Rheumatol. 2002; 20(5):647–652. [PubMed: 12412195]

44. Ogbonna AC, Clark AK, Gentry C, Hobbs C, Malcangio M. Pain-like behaviour and spinal changes in the monosodium iodoacetate model of osteoarthritis in C57Bl/6 mice. Eur J Pain. 2013; 17(4):514–526. [PubMed: 23169679]

45. Chandran P, Pai M, Blomme EA, Hsieh GC, Decker MW, Honore P. Pharmacological modulation of movement-evoked pain in a rat model of osteoarthritis. Eur J Pharmacol. 2009; 613(1–3):39–45. [PubMed: 19376109]

46. Allen KD, Adams SB Jr, Mata BA, Shamji MF, Gouze E, Jing L, et al. Gait and behavior in an IL1beta-mediated model of rat knee arthritis and effects of an IL1 antagonist. J Orthop Res. 2011; 29(5):694–703. [PubMed: 21437948]

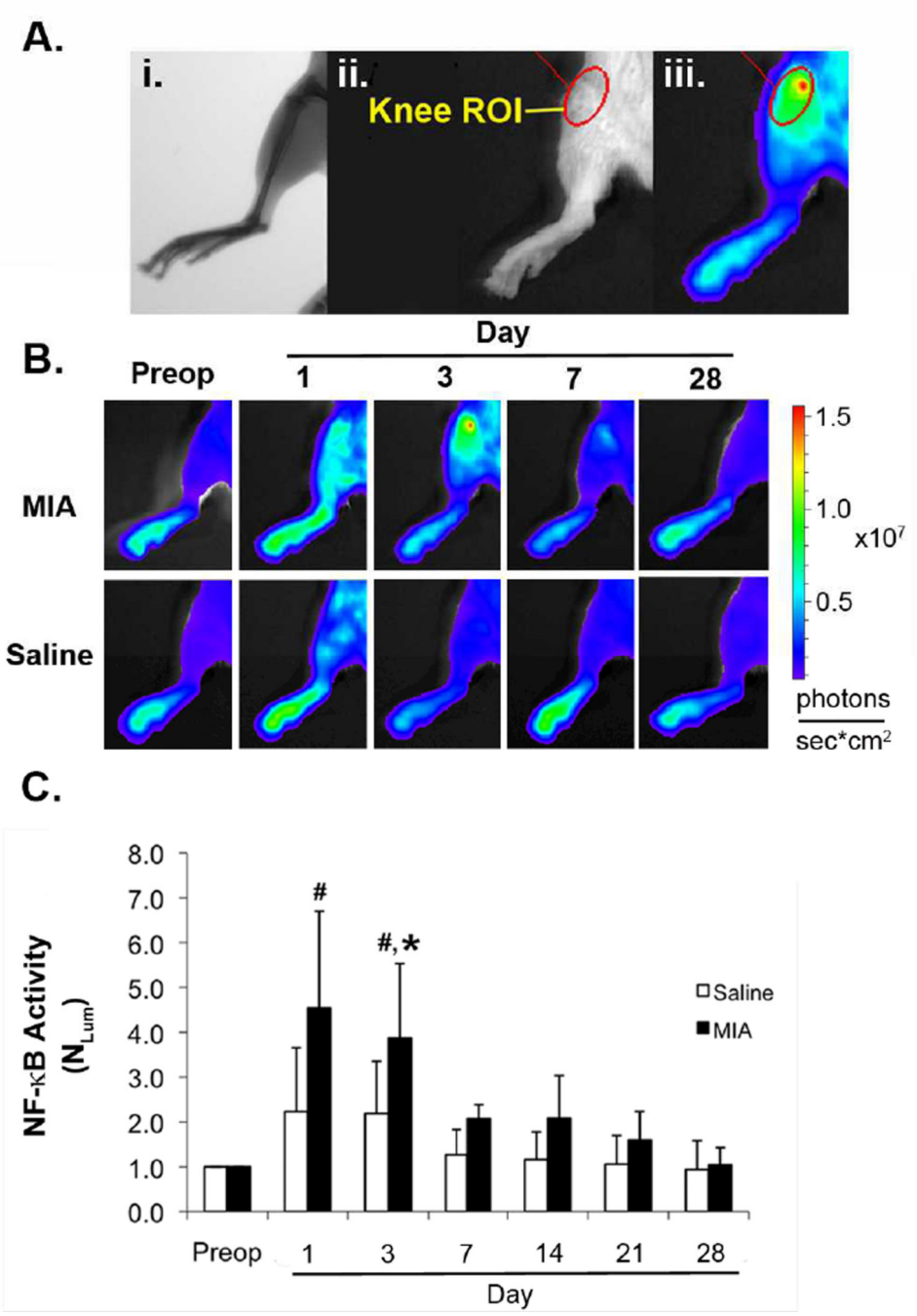

Figure 1.

(A.) Selection of knee ROI based on (i.) radiograph, (ii.) and reflected light image showing (iii.) overlay of ROI upon luminescence image of mouse limb. (B.) *In vivo* imaging of NF-κB activity in MIA and saline injected knees over 28 days. (C.) Quantitative fold-change in knee ROI luminescence (N_{LUM}) compared to preoperative levels over 28 days. ($p<0.05$, significance noted compared to preop (#) or saline (*))

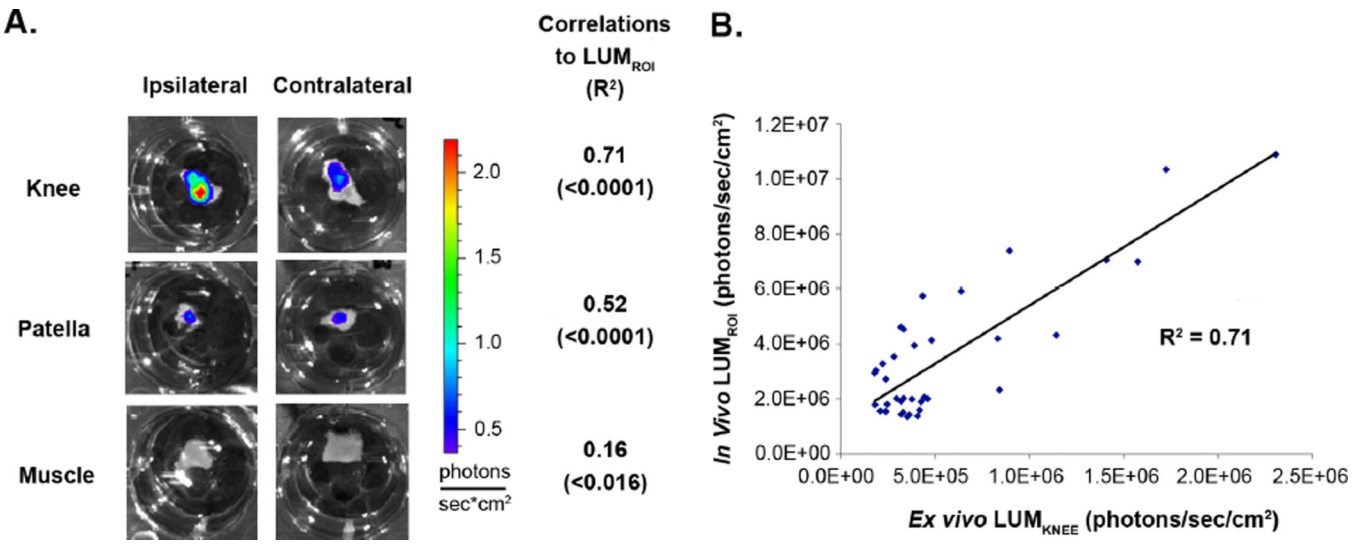

Figure 2.

(A.) *Ex vivo* luminescence imaging of ipsilateral and contralateral knee joint, patella, and adjacent muscle tissue with linear correlation coefficients to *in vivo* knee ROI luminescence (LUM_{ROI}) (p-values for correlations in parenthesis). (B.) Linear correlation between *in vivo* knee ROI luminescence (LUM_{ROI}) and *ex vivo* knee luminescence (LUM_{KNEE}).

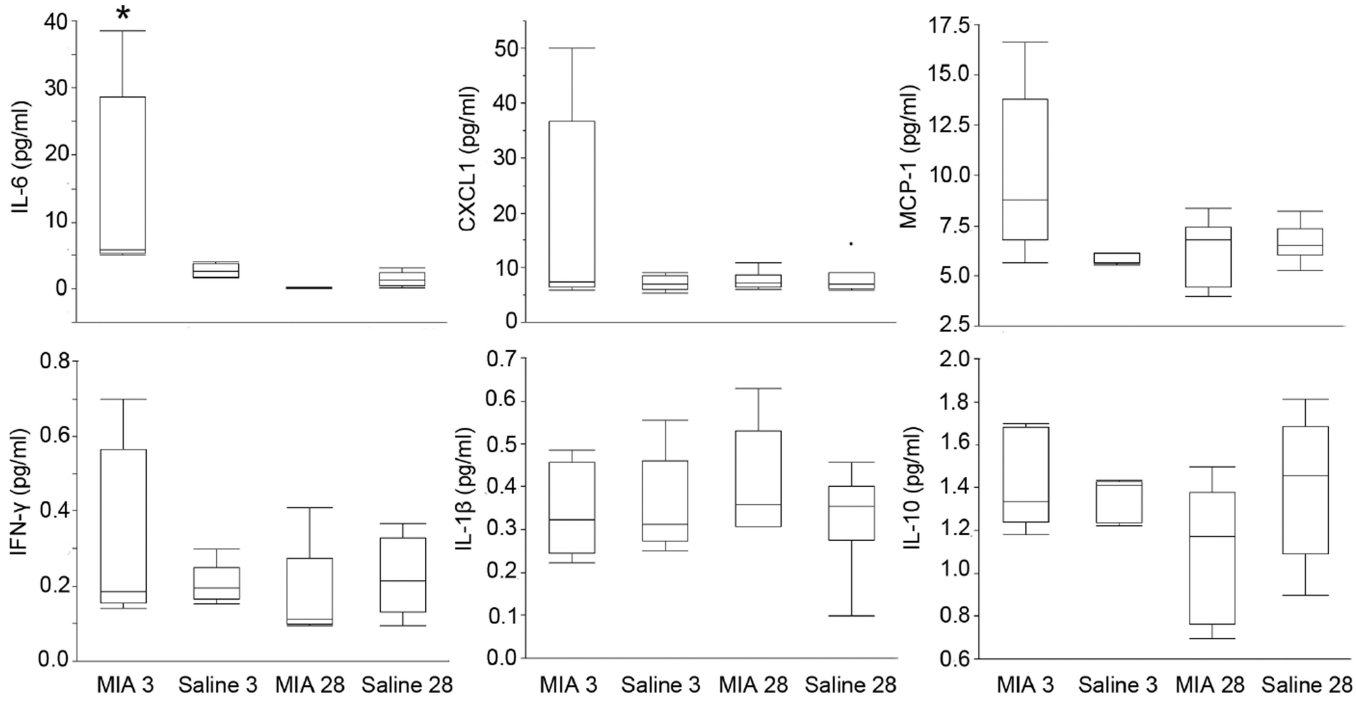

Figure 3.

Serum cytokine levels for IL-6, CXCL1, MCP-1, IFN-γ, IL-1β, and IL-10 on day 3 and 28 for MIA and saline groups. ($p<0.05$, significance noted between all groups (*) for IL-6 only)

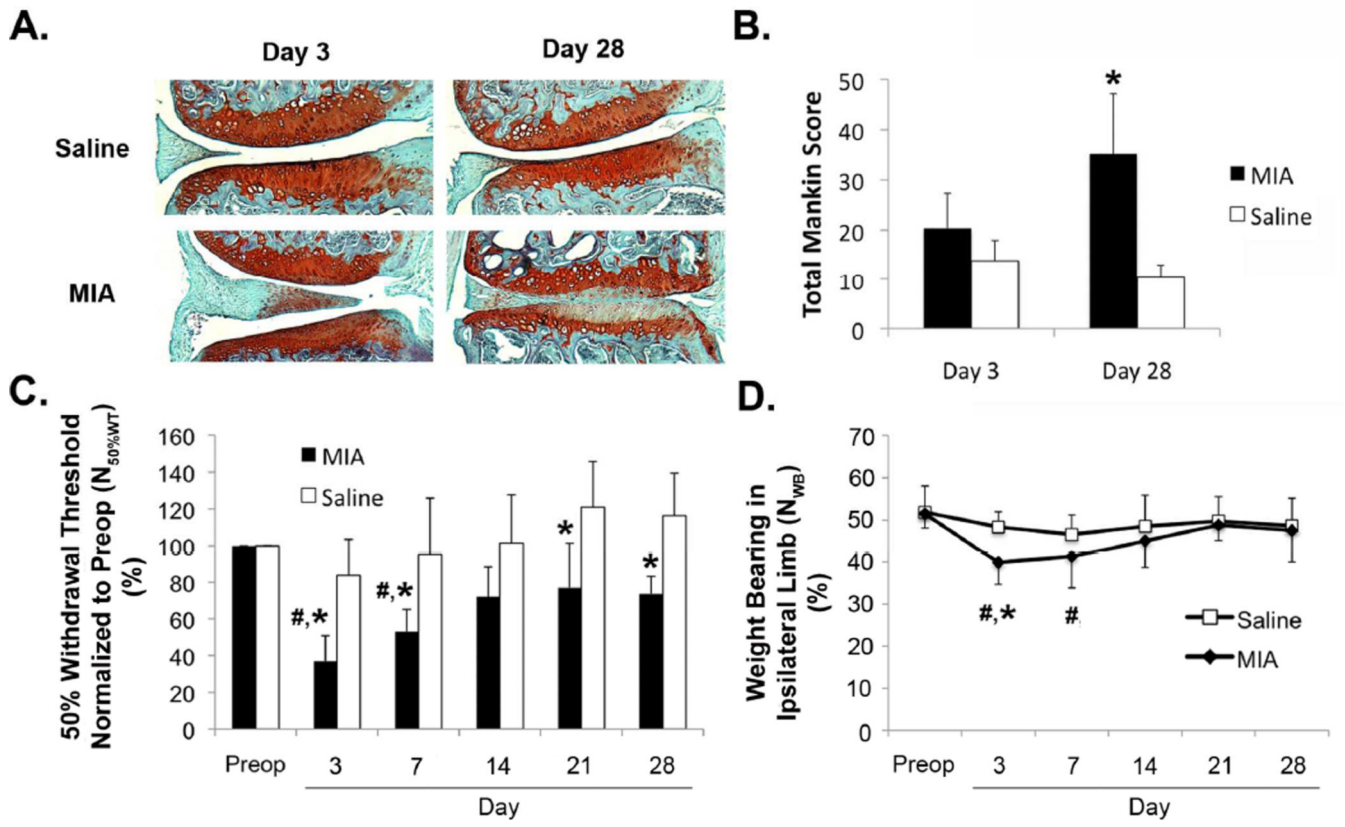

Figure 4.

(A) Representative Safranin-O/fast green stained histological sections and (B) total Mankin score from saline and MIA injected limbs on day 3 and 28 ($p<0.05$, Friedman test, significance noted compared saline (*)). (C) Normalized measures of mechanical allodynia ($N_{50\%WT}$) and (D) weight bearing (N_{WB}) in the ipsilateral limb for MIA and saline groups over 28 days. ($p<0.05$, two-way ANOVA, significance noted compared to preop (#) and saline (*)).

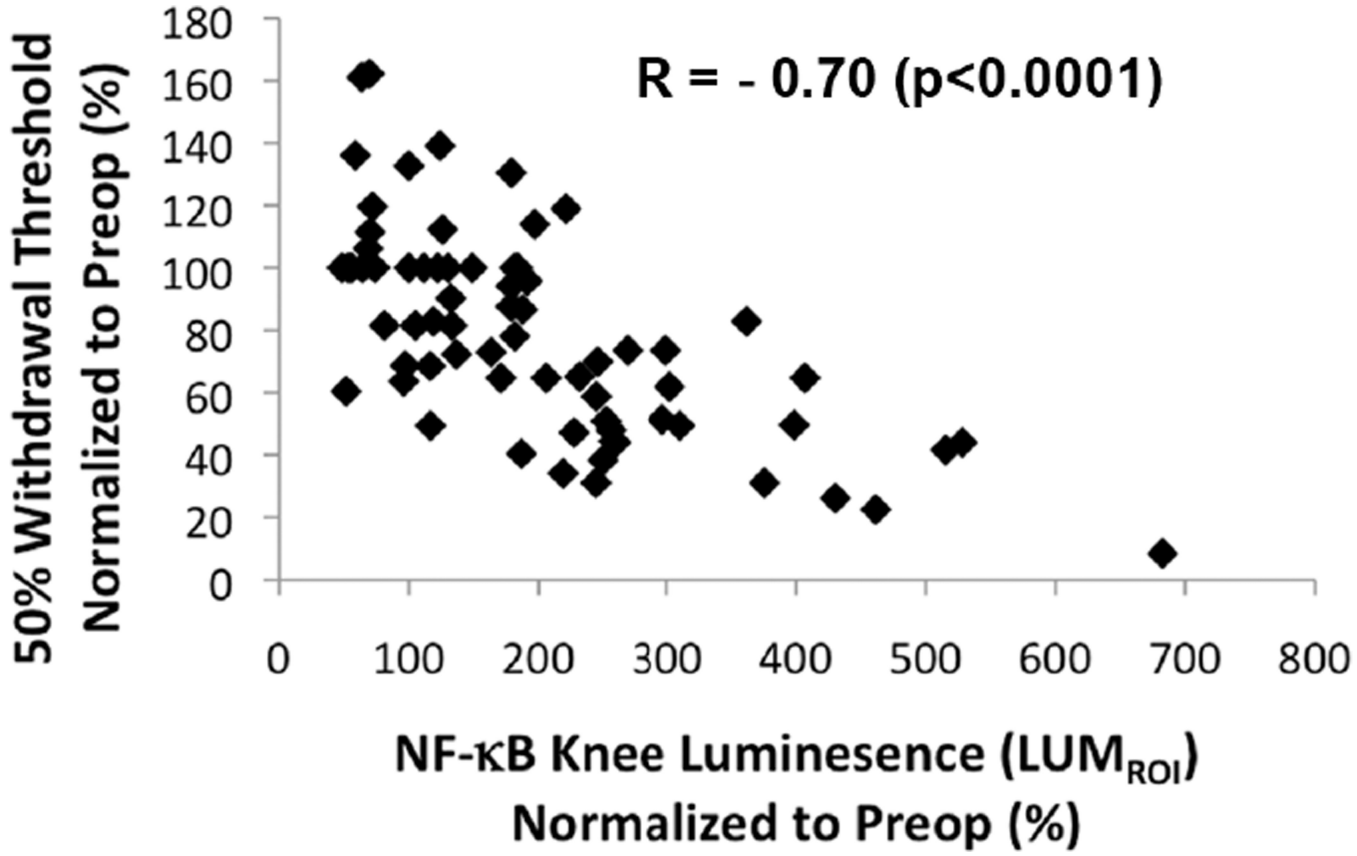

Figure 5.

50% withdrawal threshold ($N_{50\%WT}$) plotted against NF-κB activity (LUM_{ROI}) for the ipsilateral limb at all time points (Preop and days 3, 7, 14, 21, and 28).

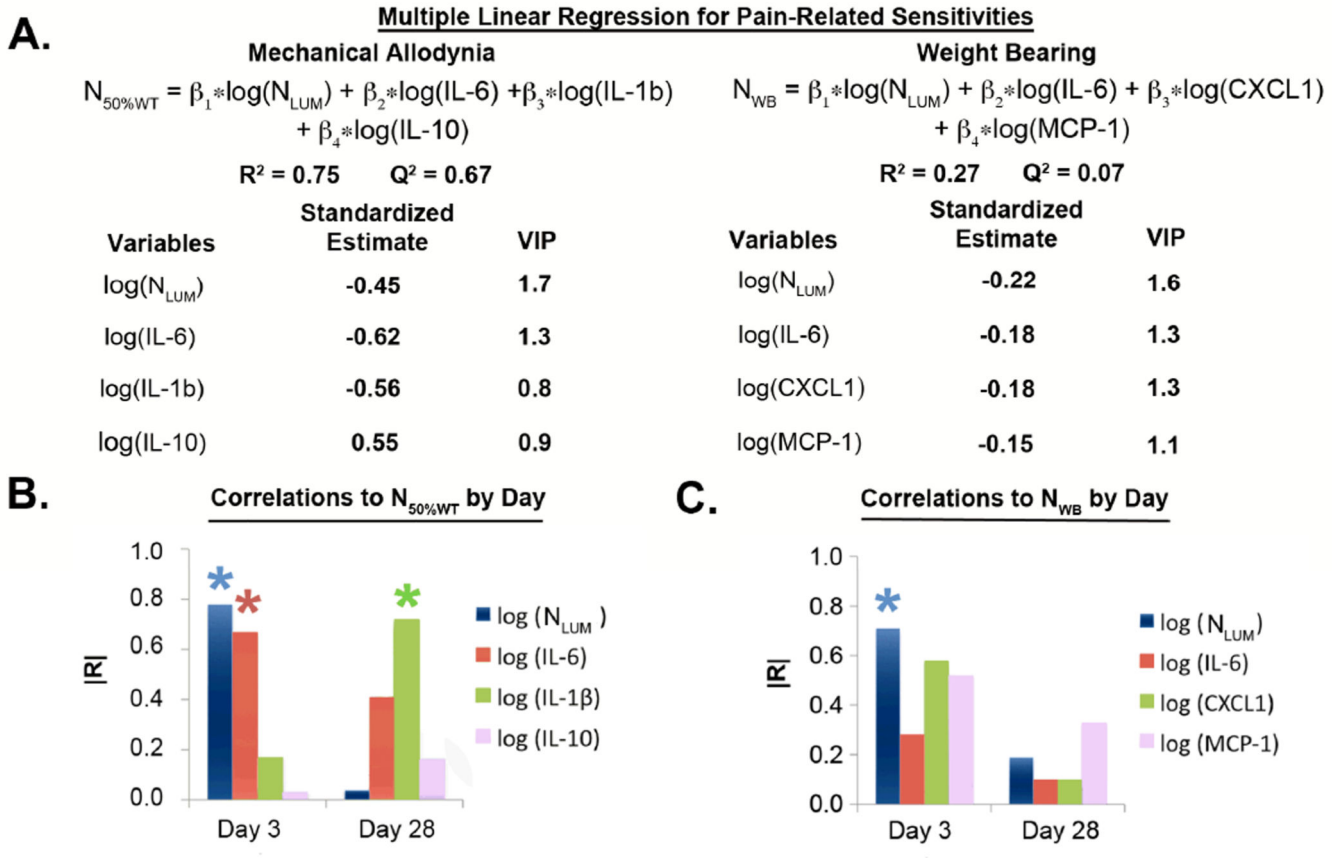

Figure 6.

(A.) Partial least squares (PLS) linear regression models created for mechanical allodynia ($N_{50\%WT}$) and weight bearing (N_{WB}). Multivariate linear correlations for variables in respective PLS linear model to (B.) mechanical allodynia and (C.) weight-bearing by day. (significant correlations denoted by *)